

# Analysis of mixed uncertainty through possibilistic inference by using error estimation of reduced order surrogate models

**T. Könecke, D. Hose, L. Frie, M. Hanss, P. Eberhard**

University of Stuttgart, Institute of Engineering and Computational Mechanics,  
Pfaffenwaldring 9, 70569 Stuttgart, Germany,  
e-mail: [tom.koenecke@itm.uni-stuttgart.de](mailto:tom.koenecke@itm.uni-stuttgart.de)

## Abstract

In the context of solving inverse problems, such as in statistical inference, an efficient repeated evaluability of a system can be achieved through methods of model order reduction. However, quantifying and adequately representing the emerging reduction error requires special techniques for combining different sources of uncertainty. In this paper, parametric finite element models are reduced through parametric model order reduction. The induced approximation error, an epistemic uncertainty, is reasonably estimated with the help of modern estimators for formulating statistical statements about the parameters to be identified. Measurement noise is also taken into account as a source of aleatory uncertainty. As a novel extension to analyzing a single source of uncertainty, the construction of a basic workflow for parameter identification in the face of both epistemic and aleatory uncertainties is presented, combining efficient error estimation techniques and possibilistic inference. The general applicability of this procedure is highlighted by two illustrative applications.

## 1 Introduction

A classical topic from the field of modeling and simulation is the inverse problem of determining input parameters of a model of interest based on measured output data through statistical inference. Of particular interest here is a realistic assessment of the influences of different types of uncertainties that need to be taken into account in the modeling process. As such, there are aleatory, i.e. random and unavoidable, uncertainties, since noisy measurements only allow statistical statements about the true parameter values. Furthermore, as uncertainty analysis typically requires a large number of model evaluations and the complexity of industrially used simulation models is increasing, it is often necessary to fall back on so-called surrogate models, to allow for an efficient evaluation. However, this model reduction itself is also a source of error, which additionally harbors uncertainties, so-called epistemic uncertainties, i.e. uncertainty due to a lack of knowledge. The challenge of dealing with the presence of uncertainties of different types and sources in reduced-order surrogate models motivates this paper.

While traditional approaches often work with probabilistic descriptions of uncertainties, newer approaches are increasingly based on alternative representations of uncertainty, being better suited for quantifying the imprecise probabilities induced by heterogeneous sources of uncertainty. In particular, possibility theory, akin to fuzzy set theory as a coarsening of classical probability theory, offers a suitable mathematical framework for making robust statements about confidence intervals of parameters, to be determined even in the case of polymorphic uncertainties of epistemic and aleatory type.

The theoretical background of the paper is given in [1], picking up some preliminary work done by [2] and [3]. Its novelty is the employment of a parametrically formulated reduced-order surrogate model to speed up the process of back propagation and then quantifying the severity of the inevitably created error by using error estimation techniques from [4] and [5], while simultaneously considering an aleatory uncertainty source in the form of noise.

The structure of the paper is laid out as follows. First, the theory behind the use of error estimators to quantify deviations stemming from model order reduction is outlined in both the time and frequency domain. Then the concepts of uncertainty quantification with imprecise probabilities and possibilistic inference for parameter identification in the presence of polymorphic uncertainty are presented. And finally, the developed methodology of parameter identification is presented along two examples, one concerning the time domain and the other concerning the frequency domain.

## 2 Error estimation in model order reduction

A mechanical system described by a linear finite element model with state vector  $\mathbf{q}(t) \in \mathbb{R}^N$ , excitation function  $\mathbf{u}(t) \in \mathbb{R}^p$ , and output behavior  $\mathbf{y}(t) \in \mathbb{R}^q$  can be formulated using the ordinary linear differential equations

$$\begin{aligned} M\ddot{\mathbf{q}}(t) + D\dot{\mathbf{q}}(t) + K\mathbf{q}(t) &= B\mathbf{u}(t), \\ \mathbf{y}(t) &= C\mathbf{q}(t), \end{aligned} \quad (1)$$

where  $M, D, K \in \mathbb{R}^{N \times N}$  are the mass, damping, and stiffness matrices,  $B \in \mathbb{R}^{N \times p}$  the input matrix, and  $C \in \mathbb{R}^{q \times N}$  the output matrix.

In order to determine the output behavior  $\mathbf{y}(t)$  of such a system, Eq. (1) must be integrated over time  $t \in [0, t_{\max}]$ . The computation time required depends not only on the length of the time interval, but also on the size of the system to be simulated. One possibility to reduce the number of equations to be solved and thus the required computing capacity is projection-based model order reduction (MOR). Its basic idea lies in the representation of the time-dependent state of a (mechanical) system  $\mathbf{q}(t) \in \mathbb{R}^N$  by the reduced state vector  $\bar{\mathbf{q}}(t) \in \mathbb{R}^n$  in a subspace. The projection of the state vector is given by

$$\mathbf{q}(t) \approx V\bar{\mathbf{q}}(t), \quad (2)$$

where  $V \in \mathbb{R}^{N \times n}$ ,  $n \ll N$  is called the projection matrix. With this, the reduced system matrices are determined as follows

$$\begin{aligned} \bar{M} &= V^T \cdot M \cdot V, \\ \bar{K} &= V^T \cdot K \cdot V, \\ \bar{D} &= V^T \cdot D \cdot V, \\ \bar{B} &= V^T \cdot B, \\ \bar{C} &= C \cdot V. \end{aligned} \quad (3)$$

Building on this, parametric MOR (PMOR) allows the reduced system matrices to be expressed as a function of some parameters, which is a critical prerequisite for rapid model evaluation for parameter identification, as evaluations at a wide variety of different parameter points are necessary. Through this method it is possible to find a reduction matrix that is not only valid for a system at an individual parameter point, but provides a sufficiently accurate approximation across parameter ranges. In this case, one speaks of a *global* PMOR approach [6]. In this contribution, the process of creating a parametrized reduced-order system will not be discussed further, please refer to [6], [7] and [8]. Instead, it will be assumed that the models are present in a parametrically reduced form.

The advantages of a faster evaluability of reduced systems are offset by an inevitable approximation error. In addition to efforts in keeping this error as low as possible, it is also important for robust MOR-based findings to be able to quantify this error. For this purpose, error estimators are used.

## 2.1 Error estimation in the time domain

In this contribution, the error estimation for simulations in the time domain is performed by a method for determining robust and guaranteed error bounds of reduced second-order systems, which has first been presented in [4]. The merits of the developed approach lie in its independence from both the integration procedure used for the numerical solution and the technique used to determine the reduction matrix  $\mathbf{V}$ . It returns a bound

$$\Delta_q(t) \geq |e(t)|, \quad (4)$$

which limits the state error  $e(t)$ , introduced by

$$\mathbf{q}(t) = \mathbf{V}_{\text{global}} \cdot \bar{\mathbf{q}}(t) + e(t). \quad (5)$$

Whenever an error estimator can warrant the validity of Eq. (4) for all points in time, its error bounds are called *guaranteed*. In addition to bounding the state error, a bound

$$\Delta_y(t) \geq |\mathbf{y}(t) - \bar{\mathbf{y}}(t)| \quad (6)$$

to the output error is of interest. This makes the error estimator usable for parameter identification based on output quantities that are measurable in experiments, as it provides bounds quantifying the output deviation between full and reduced-order systems. According to [4],

$$\Delta_y(t) = \|\mathbf{C}\|_{\mathbf{G},2} \Delta_q(t) \quad (7)$$

applies, where  $\|\mathbf{C}\|_{\mathbf{G},2}$  is the matrix norm of the output matrix with a weighting matrix  $\mathbf{G}$  which in turn can be given in the form of the mass matrix  $\mathbf{M}$ .

A property of this error estimator is the split of computation time into an initial offline-phase for  $\|\mathbf{C}\|_{\mathbf{G},2}$  and an online-phase for  $\Delta_q(t)$  which returns an error bound after the solution of every timestep.

## 2.2 Error estimation in the frequency domain

A method for finding an error metric in the frequency domain is presented in [5], the results of which do not represent mathematically guaranteed limits, but are widely used in practice and are often sufficiently good. The error

$$\varepsilon(s) = h(s) - \hat{h}(s) \quad (8)$$

is the difference between the transmission behavior  $h(s)$  of the full-order system and the transmission behavior  $\hat{h}(s)$  of a derived reduced-order system.

In order to quantify this error with an upper bound, in [5] it is proposed to calculate the frequency response of a second reduced system  $\hat{h}_C(s)$ , thus enabling the calculation of an approximative, heuristic error measure

$$\Delta_h(s) = \hat{h}(s) - \hat{h}_C(s) \gtrsim \varepsilon(s). \quad (9)$$

The second reduced-order system is referred to as the *complementary* system and should differ in its viewpoint. It is argued that in the case of a large deviation at some frequency between the two systems, which not necessarily have to be reduced with the same method, at least one of the two systems is inaccurate at this point and thus the error  $\varepsilon(s)$  has the potential to also be large. On the other hand, for frequencies where both viewpoints yield a similar response, an adequate reduction quality can be assumed. The author in [5] further argues that the creation of a complementary system when using Krylov subspace methods is

best accomplished by defining two complementary, interlocking sets of interpolation or expansion points. Since it can be assumed that the complexity of the time simulation of the reduced-order and complementary reduced-order system is approximately equivalent, a doubling of the time required for the calculation of the reduced-order system can be assumed for the determination of this error bound.

Whenever an error estimator only gives bounds, it can be assumed that no information is available about the actual realization of the error within these bounds, thus motivating the view as imprecise probabilities and possibility theory as an adequate quantification.

### 3 Uncertainty quantification and inference

The objective of the presented work is the inference of parameter distributions in a system subject to multiple sources of variously classified uncertainty. Uncertainty of polymorphic nature, reflecting both randomness and imprecision, can be quantified by imprecise probabilities. A framework for the quantification and propagation of imprecise probabilities is given by possibility theory with its measures possibility and necessity. A major advantage of possibility theory is that it allows for convenient computation by the use of possibilistic calculus, which can be implemented on a computer by using fuzzy arithmetic [9] with some additional considerations [10].

#### 3.1 Imprecise probabilities and possibility theory

The classical, frequentist theory of probability represents a precise description of the frequency of certain events, i.e. it describes the frequency of occurrence of precisely specified events. In contrast, the quantification of imprecise knowledge requires tools for dealing with imprecise probabilities, such as p-box theory, Dempster-Shafer theory of evidence or possibility theory, first formalized by Dubois and Prade [11]. Possibility theory describes the fundamental possibility that a specific event will occur, rather than its often poorly quantifiable frequency. Its core element is the elementary possibility function  $\mu$ , often also referred to as  $\pi$ , equal to a fuzzy membership function, which induces a measure of possibility

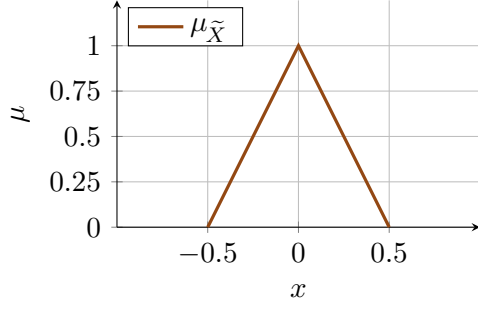
$$\Pi(x) = \sup_{\xi \leq x} \mu(\xi) \quad (10)$$

and one of necessity by

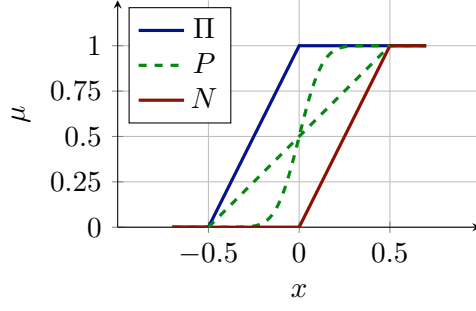
$$N(x) = \inf_{\xi > x} (1 - \mu(\xi)). \quad (11)$$

These measures exhibit the property of bounding from above and below the so-called credal set of all (consistent) probability distributions that can be assigned to such an uncertain event. Because of this property, a description of uncertainties by the use of possibilities is suitable for modeling knowledge that is based on very few observations or is characterized by fuzziness in quantification or inherent imprecision, e.g. due to measurement errors.

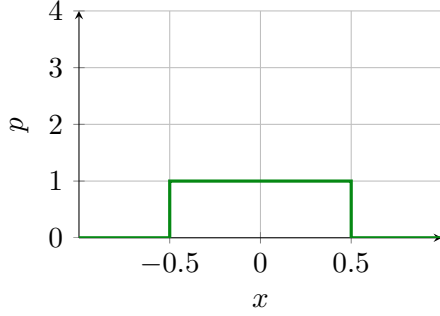
Figure 1 illustrates and explains this property by an example. It shows a triangular-shaped elementary possibility distribution  $\mu_{\tilde{X}}(x)$  (top left, orange line), used to quantify an uncertain variable  $\tilde{X}$ , as well as its derived possibility and necessity functions  $\Pi_{\tilde{X}}(x)$  and  $N_{\tilde{X}}(x)$  (top right, blue and red lines). One can see that the cumulative distribution functions (CDF) (top right, dashed green lines) for two exemplarily chosen probability density functions  $p(x)$  (bottom), here describing a uniform and a Gaussian distribution contained in the credal set belonging to  $\mu_{\tilde{X}}(x)$ , are indeed bounded from above and below, respectively. This highlights the extremely advantageous property of possibility theory that one can use only one elementary possibility function  $\mu$  together with possibilistic calculus, i.e. with a special form of fuzzy arithmetic, to describe the uncertainty of an event and to quantify the propagation of uncertainty, and that one thereby, in fact, performs at one go a calculation with a whole set of probability density functions, i.e. with all the imprecise probabilities that represent the uncertain event.



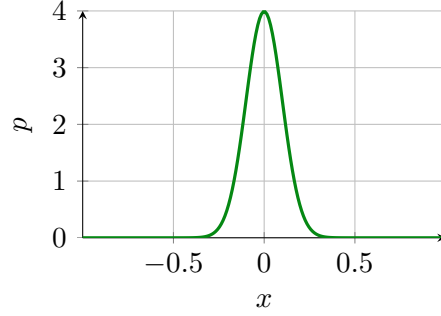
(a) A fuzzy membership function serving as an elementary possibility function



(b) The emerging possibility (blue) and necessity (red) measures bound consistent CDFs (dashed green)



(c) A uniform probability density function consistent with the elementary possibility function



(d) A Gaussian probability density function consistent with the elementary possibility function

Figure 1: Implications of a fuzzy membership function in possibility theory

In order to combine and propagate possibilistically formulated uncertain variables, they have to be encoded in an elementary possibility function. For values bounded by intervals, the possibility function can be defined as a  $\{0, 1\}$ -valued (quasi-vacuous) function, assuming a possibility value of 1 within the interval and 0 otherwise. Exactly known probabilistic distributions need to be transformed through a probability-to-possibility-transform ( $P$ - $\Pi$ -Transform) [1]. The most obvious choice for describing such values is the cumulative  $P$ - $\Pi$ -Transform, in which the value's cumulative probability function serves as its possibility function, as this automatically guarantees its inclusion in the credal set. Alternatively, the complementary function of the cumulative function can serve as possibility function [1].

Once the possibility distributions  $\mu_{\tilde{X}_i}(x_i)$  for all uncertain variables of concern are defined, the propagation  $\mu_{\tilde{Y}}$  of the uncertain variables for a mapping  $\tilde{Y} = \phi(\tilde{X})$  is obtained by

$$\mu_{\tilde{Y}}(y) = \sup_{x \in \tilde{X} : y = \phi(x)} \mu_{\tilde{X}}(x), \quad (12)$$

akin to the extension principle of fuzzy arithmetic.

In the case of propagating multiple uncertain variables, each of them characterized by a marginal possibility distribution, the joint distribution  $\mu_{\tilde{X}}(x)$  in Eq. (12) has to be found first. The construction of the joint possibility relies on different degrees of knowledge about the dependency between the individual variables. In [1] it is differentiated between the cases of unknown interaction and strong independence and computational rules of combination are provided for both cases.

### 3.2 Possibilistic Inference

Similar to statistical inference of classical, probabilistic type, possibilistic inference aims to infer a distribution of unknown parameters on the basis of noisy observations. In [1], the concept of possibilistic inference to derive confidence distributions  $\gamma$  is introduced. More precisely, given uncertain input variables  $\tilde{X}_i$  with

corresponding realizations  $x_i$ , their joint possibility distribution  $\mu_{\tilde{X}}(x)$  and an observation  $q$  of a statistical model  $\Psi$ , return a confidence distribution  $\gamma$  for uncertain model parameters  $\tilde{\theta}$  from parameter space  $\Theta$  by

$$\gamma_{\tilde{\theta}|\tilde{Q}=q}(\theta) = \sup_{x \in \tilde{X} : q = \Psi(\theta, x)} \mu_{\tilde{X}}(x) \quad \forall \theta \in \Theta. \quad (13)$$

The confidence distribution can be considered as again a membership function that encodes confidence intervals via its superlevel sets. Formally, Eq. (13) corresponds to the fuzzy extension principle, so it can be handled by the same tools. Due to this formal equality, in the following, only the symbol  $\mu$  for the classical membership function of a fuzzy set will be used for all distributions, regardless of whether it is a possibility or confidence distribution. A detailed discussion of this convention can be found in [12].

The presented method deduces a joint confidence distribution  $\gamma_{\theta_i}(\theta_i)$  for the parameters of interest. Through projection by

$$\gamma_{\theta_i}(\theta_i) = \sup_{\theta_1, \dots, \theta_{i-1}, \theta_{i+1}, \dots, \theta_n} \gamma_{\theta}(\theta), \quad (14)$$

the marginal distributions for each uncertain parameter can be obtained.

## 4 Application in the time domain

As the experiment for the time domain, a cantilever beam, as visualized in Fig. 2, is set up. It is subjected to a sinusoidally alternating force  $F$  normal to the beam axis at the free tip. The deflection  $y$  of the beam tip is measured and the task is to identify model parameters so that they mimic the behavior of the beam as well as possible. In this first, academic example, the model parameters are the stiffness and density of the beam, which is modeled on the basis of the theory of Euler and Bernoulli. Essential assumptions include its slender dimensions, i.e.  $5a \leq l$ , and its constant cross-section as well as a load along the principal inertial axis that results in small deformations relative to the beam geometry.

Here, the observation data do not stem from a physical experiment but are the result of a high-resolution numerical simulation of a beam model. The beam is discretized with 40 elements of equal size, which are connected in pairs at nodes. The parameter vector

$$\theta_{\text{ref}} = [E_{\text{ref}} \quad \rho_{\text{ref}}] = [70 \times 10^9 \frac{\text{N}}{\text{m}^2}, \quad 2750 \frac{\text{kg}}{\text{m}^3}] \quad (15)$$

is set to reference values that are considered unknown in practice and thus not available for further evaluation.

The system matrices are determined for this parameter set using the Matlab toolbox MatMorembs [13]. The system is simulated for the duration of  $t_{\text{max}} = 1$  s with a temporal resolution of  $\Delta t = 1$  ms, which corresponds to  $K = 1000$  time steps. The vertical movement of the outermost node is measured over time. A

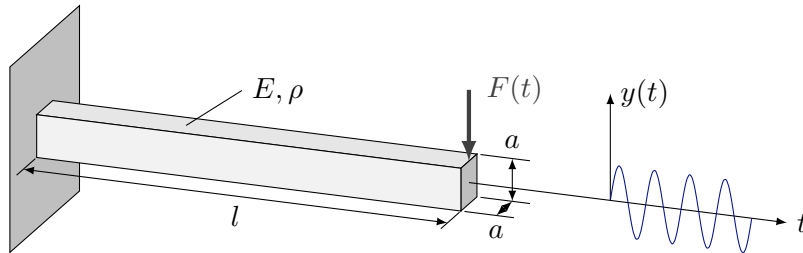


Figure 2: Cantilever beam with unknown stiffness  $E$  and density  $\rho$ , subject to a sinusoidal bending load  $F(t)$

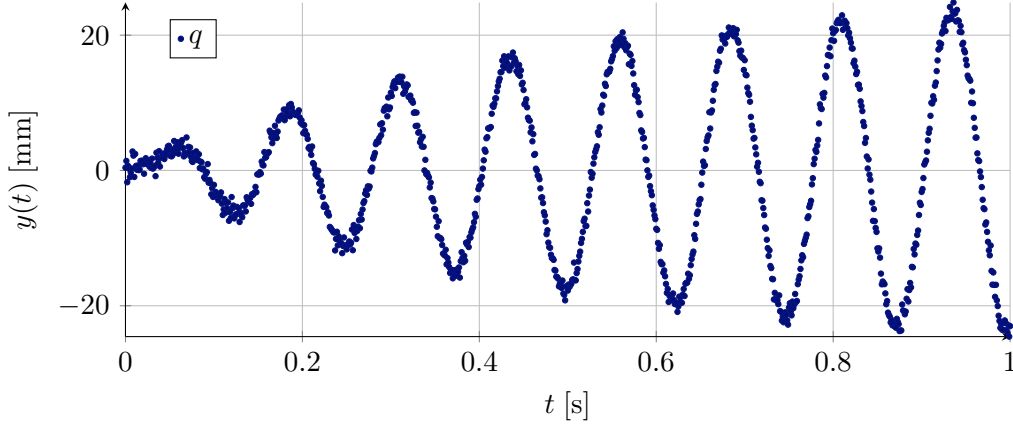


Figure 3: Observation data from the time simulation of the beam experiment

normally distributed noise with zero mean and an assumed standard deviation  $\sigma$  of 0.012 m is superimposed on the measurement signal. Figure 3 shows the measurement points of the observation  $\tilde{Q} = \mathbf{q}$  generated by these means.

It is assumed that the measurement inaccuracy occurs in the form of a normally distributed noise with zero mean and a specific standard deviation. Since the noise is independently and identically normally distributed for each time step, this error quantity can be modeled via the cumulative  $\chi^2$ -distribution

$$\mu_{\tilde{W}}(\mathbf{w}) = 1 - F_{\chi^2_K} \left( \sum_i^K \left( \frac{w_i}{\sigma} \right)^2 \right), \quad (16)$$

where  $K$  is the number of degrees of freedom, i.e. the number of summed random variables, which is the number of time steps in this case. The variable  $w_i$  is the  $i$ -th element of a time-discrete realization of the measurement noise  $\mathbf{w} \in \mathbb{R}^T$  and  $\sigma$  is the assumed standard deviation of the measurement noise.

The epistemic uncertainty, to be quantified through the error estimator, can be modeled possibilistically by the quasi-vacuous distribution

$$\mu_{\tilde{V}}(\mathbf{v}) = \begin{cases} 1 & |\mathbf{v}| \leq \Delta_y, \quad \mathbf{v} \in \mathbb{R}^T, \\ 0 & \text{else.} \end{cases} \quad (17)$$

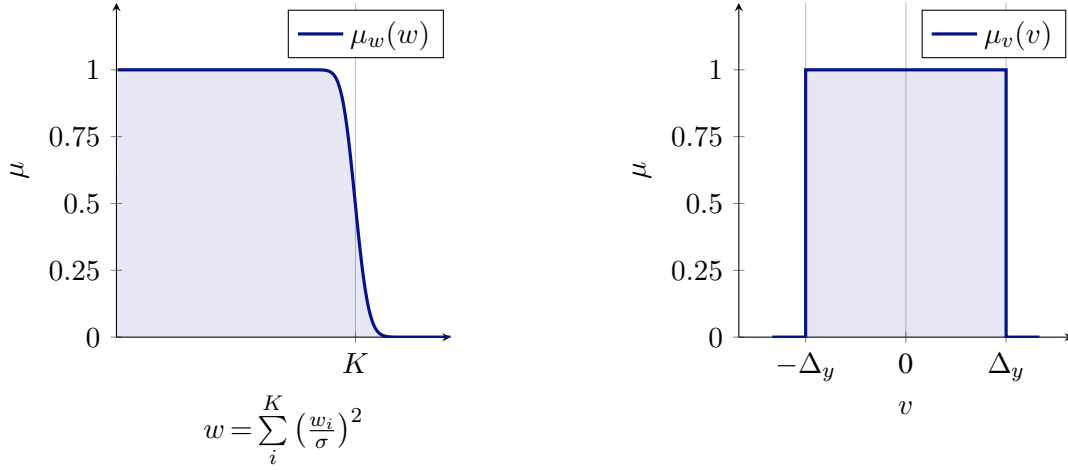
This means that the occurrence of reduction errors within the error bounds  $\Delta_y$  is possible, i.e.  $\mu_{\tilde{V}}(\mathbf{v}) = 1$ , under the assumption that an error estimator returns guaranteed bounds, and outside, it is impossible, i.e.  $\mu_{\tilde{V}}(\mathbf{v}) = 0$ . Additional information about the distribution of the error within the bounds is not available.

The membership functions of the two distributions considered as inputs for the parameter identification procedure are qualitatively shown in Figs. 4a and 4b.

Both uncertain variables  $\tilde{W}$  and  $\tilde{V}$  are modeled as additions to the model output  $y(\theta)$ , i.e. the statistical model is composed by

$$\tilde{Q} = y(\theta) + \tilde{W} + \tilde{V}. \quad (18)$$

In a first step, only the aleatory source of uncertainty shall be considered. For this, the full beam model is used for parameter identification and the epistemic error of the MOR is omitted. This option is only available if the size of the model allows for an often repeated evaluation of the system equations, which applies to the present case of a low-dimensional model. As an uncertain input quantity, only the aleatory uncertainty of the measurement noise is to be considered. Thus



(a) Possibilistic distribution of the measurement noise

(b) Possibilistic distribution of the reduction error

Figure 4: Membership functions of the considered uncertainties

$$\tilde{X} = \tilde{W}, \quad (19)$$

wherewith Eq. (13) becomes

$$\mu_{\hat{\theta}|\tilde{Q}=\mathbf{q}}(\boldsymbol{\theta}) = \sup_{\mathbf{w}:\mathbf{w}=\mathbf{q}-\mathbf{y}(\boldsymbol{\theta})} \mu_{\tilde{W}}(\mathbf{w}) = \mu_{\tilde{W}}(\mathbf{q} - \mathbf{y}(\boldsymbol{\theta})). \quad (20)$$

For each point of a set of parameters, randomly generated using Latin hypercube sampling from the parameter space, a numerical time simulation of the full beam model is carried out using the parametrically formulated system matrices. The difference between the experimental observation  $\mathbf{q}$  and the output vector  $\mathbf{y}(\boldsymbol{\theta})$  of the numerical time simulation, calculated for this parameter, is inserted into the membership function of the measurement noise in Eq. (20). The resulting membership value  $\mu$  is stored together with  $\boldsymbol{\theta}$  in a tuple  $(\boldsymbol{\theta}, \mu)$ , a so-called  $\mu$ -cluster. The values determined with the full model are shown in blue in Fig. 5.

As discussed, evaluating the full system for every parameter point is not feasible for more complex models. Thus, as a next step, a model order reduction is applied, introducing another uncertain value, namely the discrepancy between the time domain simulations of the full and the reduced-order system.

The membership function  $\mu_{\tilde{X}}(x)$  for the uncertain variables  $\tilde{X}$  is replaced by the joint membership function  $\mu_{\tilde{W},\tilde{V}}(\mathbf{w}, \mathbf{v})$  of the two uncertain inputs  $\tilde{W}$  and  $\tilde{V}$ , allowing Eq. (13) to be rewritten as

$$\mu_{\hat{\theta}}(\boldsymbol{\theta}) = \sup_{\mathbf{w},\mathbf{v}:\mathbf{q}=\Psi(\boldsymbol{\theta},(\mathbf{w},\mathbf{v}))} \mu_{\tilde{W},\tilde{V}}(\mathbf{w}, \mathbf{v}). \quad (21)$$

According to [12], the joint distribution function  $\mu_{\tilde{W},\tilde{V}}(\mathbf{w}, \mathbf{v})$  can be calculated by using the minimum operator through

$$\mu_{\tilde{W},\tilde{V}}(\mathbf{w}, \mathbf{v}) = \min_{\mathbf{w},\mathbf{v}} \{\mu_{\tilde{W}}(\mathbf{w}), \mu_{\tilde{V}}(\mathbf{v})\} \quad (22)$$

due to the property of  $\mu_{\tilde{V}}$  being quasi-vacuous. Therefore, Eq. (21) extends to

$$\mu_{\hat{\theta}}(\boldsymbol{\theta}) = \sup_{\mathbf{w},\mathbf{v}:\mathbf{q}=\Psi(\boldsymbol{\theta},(\mathbf{w},\mathbf{v}))} \min_{\mathbf{w},\mathbf{v}} \{\mu_{\tilde{W}}(\mathbf{w}), \mu_{\tilde{V}}(\mathbf{v})\}. \quad (23)$$



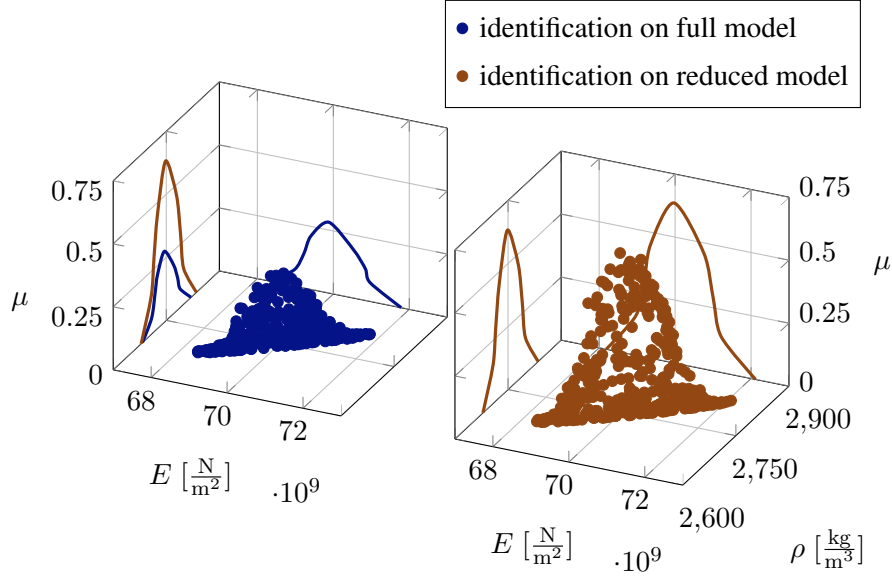


Figure 5: Joint and marginal parameter confidence distributions of the parameters  $E$  and  $\rho$

The membership function  $\mu_{\tilde{\mathcal{V}}}(\mathbf{v})$  can only take on two values. For  $\mathbf{v} \in \mathbb{V}$  it is 1. Clearly,  $\mathbb{V}$  corresponds to the space of exactly all those vectors  $\mathbf{v}$  that lie within the interval of the error bounds  $[-\Delta_y, \Delta_y]$ . In this case, due to the minimum operator, only the membership function  $\mu_{\tilde{\mathcal{W}}}(\mathbf{w})$  is relevant for the output value. For all other  $\mathbf{v}$  the minimum takes the value  $\mu_{\tilde{\mathcal{V}}}(\mathbf{v}) = 0$ . Accordingly, Eq. (23) can be simplified to

$$\mu_{\hat{\theta}}(\boldsymbol{\theta}) = \sup_{\mathbf{v} \in \mathbb{V} : \mathbf{q} = \Psi(\boldsymbol{\theta}, (\mathbf{w}, \mathbf{v}))} \mu_{\tilde{\mathcal{W}}}(\mathbf{w}). \quad (24)$$

The additive relation from Eq. (18) is used to write

$$\mathbf{w}(\mathbf{v}) = \mathbf{q} - \bar{\mathbf{y}}(\boldsymbol{\theta}) - \mathbf{v} \quad (25)$$

as a function of  $\mathbf{v}$ , where the vector  $\bar{\mathbf{y}}(\boldsymbol{\theta}) \in \mathbb{R}^K$  is the output vector of the reduced deterministic model. Consequently, one obtains

$$\mu_{\hat{\theta}}(\boldsymbol{\theta}) = \sup_{\mathbf{v} \in \mathbb{V} : \mathbf{q} = \Psi(\boldsymbol{\theta}, (\mathbf{w}, \mathbf{v}))} \mu_{\tilde{\mathcal{W}}}(\mathbf{q} - \bar{\mathbf{y}}(\boldsymbol{\theta}) - \mathbf{v}). \quad (26)$$

Finally, since the cumulative  $\chi^2$ -distribution function underlying the function  $\mu_{\tilde{\mathcal{W}}}(\mathbf{w})$  is monotonically decreasing, minimizing the argument  $\sum w_i^2$  consequently maximizes the distribution function. Thus,

$$\mu_{\hat{\theta}}(\boldsymbol{\theta}) = \mu_{\tilde{\mathcal{W}}}\left(\inf_{\mathbf{v} \in \mathbb{V} : \mathbf{q} = \Psi(\boldsymbol{\theta}, (\mathbf{w}, \mathbf{v}))} \sum_i^K (q_i - \bar{y}_i(\boldsymbol{\theta}) - v_i)^2\right) \quad (27)$$

proves equivalent to Eq. (26), where the inner expression can be efficiently solved numerically as a quadratic optimization problem.

Again, a random set of points is generated from the parameter space  $\Theta$  and the system equations are set up for each point using the parametrically formulated system matrices. In addition, a reduced system for each parameter point is calculated using a parameter-independent global reduction matrix, obtained through Krylov reduction. Then, the error estimator from [4] is initialized with the system matrices of the full system, the reduction matrix and the excitation function. The time simulation of the reduced system is performed

over a duration of  $t_{\max} = 1$  s with a temporal resolution of  $\Delta t = 1$  ms. The error estimator calculates a bound  $\Delta_y$  for each time step, which bounds the deviation of the reduced solution to the full solution at that point. To evaluate the inner term of Eq. (27), the function `quadprog` implemented in Matlab is used to find a vector  $\boldsymbol{v}$  within the error bound  $\Delta_y$  that minimizes the term. Finally, the resulting vector  $\boldsymbol{v}$  is used to compute the infimum, which is substituted into the distribution function  $\mu_{\tilde{\mathcal{W}}}(\boldsymbol{w})$ . Due to the significant computational overhead in the initialization phase of the error estimator, a reduction of the calculation time by the applied model order reduction only occurs upwards of some reduction magnitude. The resulting confidence distribution for the parameter vector  $\boldsymbol{\theta}$ , identified using the reduced model, is illustrated in orange in Fig. 5. At first sight, the confidence distributions stemming from the full- and reduced-order model appear to be similar. Taking a comparative look at the marginal distributions for the stiffness parameter  $E$ , however, reveals a significant difference in the accuracy of the identification. The marginal distributions differ in their width and maximum. A trade-off between the speed of parameter identification and its accuracy can be observed.

## 5 Application in the frequency domain

As an example for an application in the frequency domain, a model of a disc brake is investigated next. In [8], a model of a disc brake for the analysis of brake squeal is presented, which is used in this investigation. The parameter selected for identification is, in this example, the disc speed  $\Omega$ . A visualization of the brake model is provided in Fig. 6.

There are several nonlinear effects to be considered in the brake model due to contact and rotational influences. For a detailed explanation, please refer to [8]. The linearized parametrized system can then be modeled by

$$\begin{aligned} M\ddot{\boldsymbol{q}} + \hat{\boldsymbol{D}}(\Omega)\dot{\boldsymbol{q}} + \hat{\boldsymbol{K}}(\Omega)\boldsymbol{q} &= \boldsymbol{B}\boldsymbol{u}, \\ \boldsymbol{y} &= \boldsymbol{C}\boldsymbol{q} \end{aligned} \quad (28)$$

with the matrices  $\hat{\boldsymbol{D}}(\Omega)$  and  $\hat{\boldsymbol{K}}(\Omega)$  being parameter-dependent. The corresponding transfer function is given by

$$\boldsymbol{H}(\omega, \Omega) = \boldsymbol{C} \left( -\omega^2 \boldsymbol{M} + i\omega \hat{\boldsymbol{D}}(\Omega) + \hat{\boldsymbol{K}}(\Omega) \right)^{-1} \boldsymbol{B}. \quad (29)$$

In addition to a full model with  $N = 4669$  degrees of freedom, a parametrically reduced model with  $n = 100$  degrees of freedom is derived using Krylov reduction.

The displacement of the excitation point and the measurement point shall serve as the input and output values for the transfer behavior of the system. In contrast to the previous section, the system response in the frequency domain is now object of the parameter identification. The frequency response is determined numerically for the range from 0 to 500 Hz. Again, first, only an aleatory source of uncertainty in the form of noise on the measured data in the experiment is introduced. It is assumed to behave in the same way as in the time-domain case, i.e. following a normal distribution with zero mean and an assumed variance. The result of the experiment can be seen in Fig. 7.

Based on this data, the full model of the brake system is used to generate predictions and evaluate them with Eq. (27) according to the proposed method. The resulting parameter distribution is shown in Fig. 8. Subsequently, two reduced-order models are derived with global reduction matrices stemming from Krylov reduction with interlacing expansion points. The possibilistic inference is carried out again using the aforementioned error heuristic from [5], providing the bounds. This parameter distribution is also shown in Fig. 8.

Again, a deterioration in identification accuracy is observed at the benefit of a significant speedup in computation time.

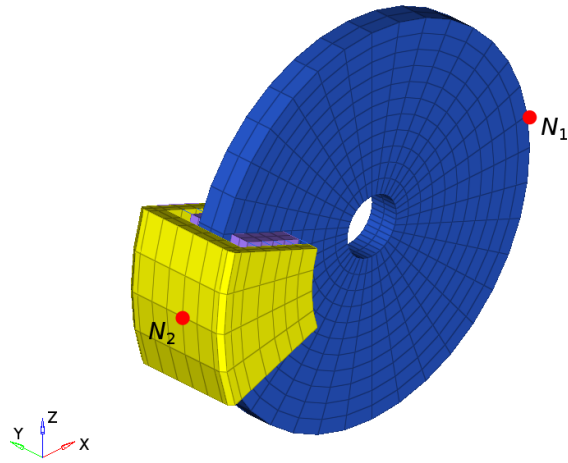


Figure 6: Visualization of the disc brake system from [8]. Excitation and measurement points are marked in red.

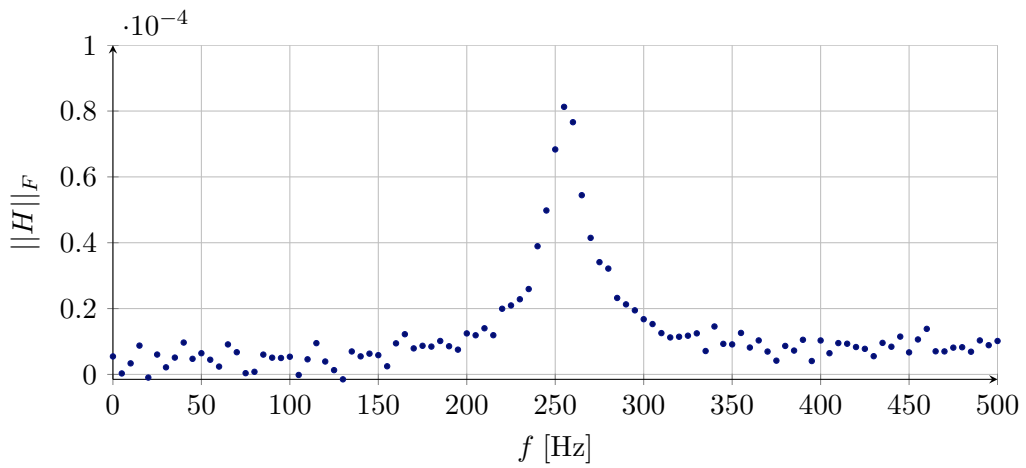


Figure 7: Noisy observation data  $q$  from the frequency response of the disc brake system experiment

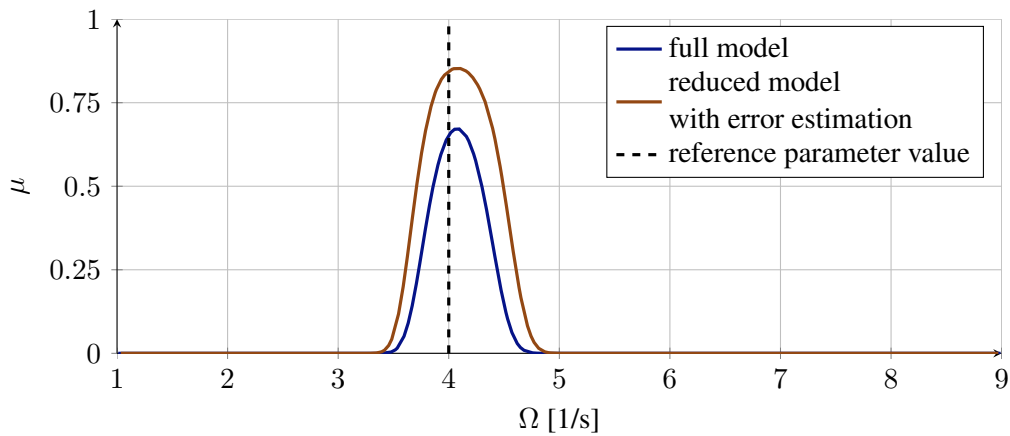


Figure 8: Confidence distributions for the identification of the rotational speed  $\Omega$  of the disc brake system

## 6 Conclusion

In this paper, a possibilistically formulated inference method for parameter identification under uncertainty is presented and applied to two different problems: one considered in the time-domain and one in the frequency domain. The method involves the comparison of an experimental observation with the results of an evaluation of a numerical model carried out under different model parameters. In this context, tools for uncertainty quantification by possibility theory and existing error estimation techniques are used. It can be shown that the quantitative inclusion of both aleatory and epistemic uncertainties is feasible.

An important property of the developed inference method is its independence of the underlying experimental data source and especially to the error estimator used. Due to the modular implementation of the method, any algorithm capable of calculating error bounds in both the time or frequency domain can be used by modifying only a few lines of code. This modular applicability is highlighted by an exemplary application to the time simulation of an oscillating beam as well as to the frequency analysis of an automotive disc brake. A trade-off can be observed, where the appropriate consideration of model order reduction error degrades the identification quality at the benefit of faster computation times.

A major contribution of this work consists not only of applying methods of uncertainty analysis to polymorphic uncertainties and using an error estimator to quantify epistemic uncertainty, but also by creating a structured procedure for the practical application of possibilistic inference methods for parameter identification, illustrated by examples.

Points of contact lie in the extension of the developed method to other problem areas in which the parameter identification subject to uncertainties could provide added value. These could also include problems outside the numerical simulation of mechanical systems, such as in the field of machine learning, in which the detection of complex relationships on the basis of large amounts of data is ultimately also based on the identification of suitable model parameters. In addition, the emergence of better methods for the robust estimation of model order reduction errors, such as indicated in [14], will rapidly lead to a higher effectiveness of the developed method.

## Acknowledgements

The authors gratefully acknowledge the support provided by the German Research Foundation (DFG) in the framework of the research project no. 319924547 (HA2798/9-2) as well as the support within the framework of the EVOLVE research project (FKZ 20A1902C) funded by the German Federal Ministry for Economic Affairs and Climate Action.

Supported by:



Federal Ministry  
for Economic Affairs  
and Climate Action

on the basis of a decision  
by the German Bundestag

## References

- [1] D. Hose and M. Hanss, “A universal approach to imprecise probabilities in possibility theory,” *International Journal of Approximate Reasoning*, vol. 133, pp. 133–158, 2021.
- [2] A. Brauchler, D. Hose, P. Ziegler, M. Hanss, and P. Eberhard, “Distinguishing geometrically identical instruments: possibilistic identification of material parameters in a parametrically model order reduced finite element model of a classical guitar,” *Journal of Sound and Vibration*, vol. 535, p. 117071, 2022.
- [3] D. Hose and M. Hanss, “Towards a general theory for data-based possibilistic parameter inference,” in *Proceedings of the 3rd International Conference on Uncertainty Quantification in Computational Sciences and Engineering in Crete (Greece)*, 2019.
- [4] D. Grunert, J. Fehr, and B. Haasdonk, “Well-scaled, a-posteriori error estimation for model order reduction of large second-order mechanical systems,” *ZAMM Journal of Applied Mathematics and Mechanics*, vol. 100, no. 8, p. e201900186, 2020.

- [5] E. J. Grimme, “Krylov projection methods for model reduction,” Ph.D. dissertation, University of Illinois at Urbana-Champaign, 1997.
- [6] B. Fröhlich, D. Hose, O. Dieterich, M. Hanss, and P. Eberhard, “Uncertainty quantification of large-scale dynamical systems using parametric model order reduction,” *Mechanical Systems and Signal Processing*, vol. 171, p. 108855, 2022.
- [7] P. Benner, S. Gugercin, and K. Willcox, “A survey of projection-based model reduction methods for parametric dynamical systems,” *SIAM Review*, vol. 57, no. 4, pp. 483–531, 2015.
- [8] F. Matter, B. Fröhlich, I. Iroz, and P. Eberhard, “Investigations of disc brake squeal using model order reduction approaches for the complex eigenvalue analysis,” in *27th Annual Congress of the International Institute of Acoustics and Vibration (IIAV)*, July 2021.
- [9] M. Hanss, *Applied Fuzzy Arithmetic: An Introduction with Engineering Applications*. Springer, Berlin, 2005.
- [10] D. Hose and M. Hanss, “Possibilistic calculus as a conservative counterpart to probabilistic calculus,” *Mechanical Systems and Signal Processing*, vol. 133, p. 106290, 2019.
- [11] D. Dubois and H. Prade, *Possibility Theory: An Approach to Computerized Processing of Uncertainty*. Plenum Press, New York, 1988.
- [12] D. Hose, *Possibilistic Reasoning with Imprecise Probabilities: Statistical Inference and Dynamic Filtering*. Aachen: Shaker, 2022, vol. 74.
- [13] J. Fehr, D. Grunert, P. Holzwarth, B. Fröhlich, N. Walker, and P. Eberhard, “Morembs—a model order reduction package for elastic multibody systems and beyond,” in *Reduced-Order Modeling (ROM) for Simulation and Optimization: Powerful Algorithms as Key Enablers for Scientific Computing*, W. Keiper, A. Milde, and S. Volkwein, Eds. Cham: Springer International Publishing, 2018.
- [14] A. Schmidt, D. Wittwar, and B. Haasdonk, “Rigorous and effective a-posteriori error bounds for non-linear problems—application to rb methods,” *Advances in Computational Mathematics*, vol. 46, no. 2, pp. 1–30, 2020.